Structure of Crumbs tail in complex with the PALS1 PDZ–SH3–GK tandem reveals a highly specific assembly mechanism for the apical Crumbs complex

Youjun Li[a,1], Zhiyi Wei[a,b,c,1], Yan Yan[a,b], Qingwen Wan[d], Quansheng Du[d], and Mingjie Zhang[a,b,2]

[a]Division of Life Science, State Key Laboratory of Molecular Neuroscience and [b]Center of Systems Biology and Human Health, School of Science and Institute for Advanced Study, Hong Kong University of Science and Technology, Clear Water Bay, Kowloon, Hong Kong, China; [c]Department of Biology, South University of Science and Technology of China, Shenzhen 518055, China; and [d]Department of Neuroscience and Regenerative Medicine, Medical College of Georgia, Georgia Regents University, Augusta, GA 30912

Edited by Thomas C. Südhof, Stanford University School of Medicine, Stanford, CA, and approved October 17, 2014 (received for review August 27, 2014)

The Crumbs (Crb) complex, formed by Crb, PALS1, and PATJ, is evolutionarily conserved in metazoans and acts as a master cell-growth and -polarity regulator at the apical membranes in polarized epithelia. Crb intracellular functions, including its direct binding to PALS1, are mediated by Crb's highly conserved 37-residue cytoplasmic tail. However, the mechanistic basis governing the highly specific Crb–PALS1 complex formation is unclear, as reported interaction between the Crb tail (Crb-CT) and PALS1 PSD-95/DLG/ZO-1 (PDZ) domain is weak and promiscuous. Here we have discovered that the PDZ–Src homolgy 3 (SH3)–Guanylate kinase (GK) tandem of PALS1 binds to Crb-CT with a dissociation constant of 70 nM, which is ∼100-fold stronger than the PALS1 PDZ–Crb-CT interaction. The crystal structure of the PALS1 PDZ–SH3–GK–Crb-CT complex reveals that PDZ–SH3–GK forms a structural supramodule with all three domains contributing to the tight binding to Crb. Mutations disrupting the tertiary interactions of the PDZ–SH3–GK supramodule weaken the PALS1–Crb interaction and compromise PALS1-mediated polarity establishment in Madin–Darby canine kidney (MDCK) cysts. We further show that specific target binding of other members of membrane-associated guanylate kinases (MAGUKs) (e.g., CASK binding to neurexin) also requires the presence of their PDZ–SH3–GK tandems.

cell polarity | supramodule | MAGUK | PBM | Stardust

A principal property of epithelial cells is their apical–basal polarity, which contributes to cell morphology, directional vesicle transportation, and specific localization of proteins and lipids (1–3). The establishment and maintenance of apical–basal cell polarity is governed by several sets of highly conserved protein complexes collectively referred to as polarity complexes (1–4). Extensive genetic and cell biology investigations in the last two decades have identified three protein complexes, namely the Crb–PALS1–PATJ complex, PAR3–PAR6–aPKC complex, and DLG–LGL–Scribble complex, as the principal cell-polarity regulators (5–10), although direct evidence supporting formation of the DLG–LGL–Scribble tripartite complex at the biochemical level is lacking. These complexes act cooperatively in defining the apical–basal border and maintaining the apical–basal axis of epithelia in diverse tissues. Among these complexes, only Crb is a transmembrane protein and known as a determinant of apical–basal cell polarity in most epithelial cells (11–13). In early *Drosophila* embryos, dysfunction mutations of Crb lead to the loss of apical-membrane identity, and overexpression of Crb causes expansion of apical-membrane size at the expense of basolateral membranes (14, 15). Recently, Crb has also been identified as controlling cell growth by functioning as an upstream regulator of the Hippo pathway (16–18).

As a type I transmembrane protein, Crb is composed of an extracellular region, a transmembrane domain, and a 37-residue highly conserved cytoplasmic tail (Crb-CT; Fig. 1*A*), which contains a protein 4.1/Ezrin/Radixin/Moesin (FERM)-binding motif (FBM), a PSD-95/DLG/ZO-1 (PDZ)-binding motif (PBM), and a potential aPKC phosphorylation site (19–22). In certain tissues, expression of transmembrane domain-tethered Crb-CT alone can rescue the *crb* mutant phenotype similar to that of full-length Crb (15, 19), indicating that the cytoplasmic tail plays a crucial role for the functions of Crb. A *Drosophila* Crb allele, crb^{8F105}, encoding a mutant protein that retains FBM but lacks the C-terminal 23 amino acids, develops similar embryonic defects as the *Crb* null allele (14, 20), pointing to the determinant role of the C-terminal PBM-containing sequence of Crb in embryonic development.

The formation of the Crb complex requires direct and specific interaction between Crb-CT and PALS1 (Stardust in *Drosophila*) (23–26). It is well-established that both the extreme C-terminal PBM of Crb-CT (i.e., the "ERLI" sequence) and the PALS1 PDZ domain are required for the Crb–PALS1 interaction (23). However, both large-scale, systematic PDZ–target interaction screening studies (27, 28) and many individual studies (ref. 29 and references therein) have shown that interactions between an isolated PDZ domain and a short PBM sequence of 4–10 residues are often weak (K_d of a few to tens micromolar) and have low specificity. This is also true for the Crb-CT and PALS1-PDZ, as we demonstrate in this study. Such promiscuous PDZ–target interactions are at odds with highly specific cellular functions known for many PDZ domain proteins as well as their binding targets, including the Crb–PALS1 interaction (23, 24, 30). An

Significance

The Crumbs–PALS1–PATJ complex is vital for the development and maintenance of the polarity of diverse tissues. Defects in Crumbs–PALS1–PATJ complex formation are known to cause diseases such as cancer and blindness. The highly conserved cytoplasmic tail of the transmembrane protein Crumbs is responsible for the apical targeting of the Crumbs–PALS1–PATJ complex. However, the molecular basis governing the formation of the highly specific Crumbs–PALS1 complex is poorly understood. We discovered that the PDZ–SH3–GK tandem of PALS1 forms a structural supramodule interacting with the large part of the Crumbs tail with high affinity and specificity, supporting the apical–basal polarity of epithelial cells. Our work suggests that formation of the PDZ–SH3–GK supramodule is a general property of MAGUKs for recognizing specific targets.

Author contributions: Y.L., Z.W., and M.Z. designed research; Y.L., Z.W., Q.W., and Q.D. performed research; Y.Y. contributed new reagents/analytic tools; Y.L., Z.W., Y.Y., Q.W., Q.D., and M.Z. analyzed data; and Y.L., Z.W., Q.D., and M.Z. wrote the paper.

The authors declare no conflict of interest.

This article is a PNAS Direct Submission.

Data deposition: The crystallographic data reported in this paper have been deposited in the Protein Data Bank, www.pdb.org (PDB ID code 4WSI).

[1]Y.L. and Z.W. contributed equally to this work.

[2]To whom correspondence should be addressed. Email: mzhang@ust.hk.

This article contains supporting information online at www.pnas.org/lookup/suppl/doi:10.1073/pnas.1416515111/-/DCSupplemental.

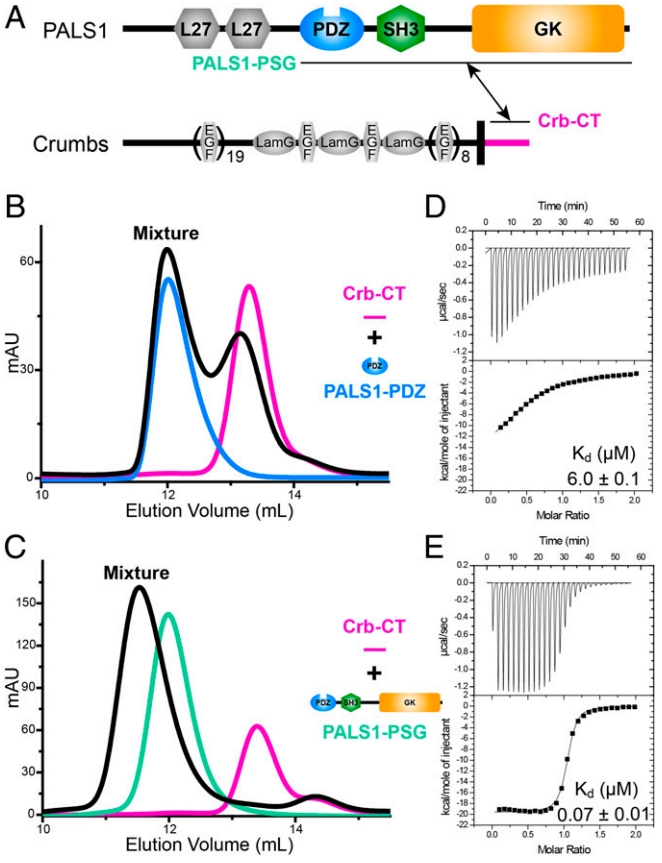

Fig. 1. PALS1-PSG binds to Crb-CT with high affinity. (*A*) Schematic diagrams of the domain organization of PALS1 and Crb. The PALS1-PSG–Crb-CT interaction is indicated by a two-way arrow. Note that, unlike Crb1 and Crb2, vertebrate Crb3 lacks the large extracellular domains. (*B* and *C*) Analytical gel filtration chromatography showing the binding profiles of Crb-CT to PALS1-PDZ (*B*) and PALS1-PSG (*C*). mAU, UV absorbance at 280 nm. (*D* and *E*) Isothermal titration calorimetry (ITC)-based measurements quantifying the binding of Crb-CT to PALS1-PDZ (*D*) and PALS1-PSG (*E*).

emerging theme is that many PDZ domains can "collaborate" with their extension sequences at the two termini (referred to as PDZ extensions) or their neighboring domain(s) (i.e., forming so-called PDZ supramodules) to establish their highly specific target-binding capacities (29). It has been shown that either a single point mutation in the SH3 domain or deletion of both the SH3 and GK domains of PALS1 compromises PALS1-mediated polarization of MDCK cells (31), although the underlying mechanism is unclear.

Given the paramount roles of both Crb and PALS1 in cell polarity and growth in diverse tissues, here we investigated the mechanistic basis governing the specific interaction between these two proteins. We show that the PDZ–SH3–GK (PSG) tandem of PALS1 binds to Crb-CT with ∼100-fold higher affinity than the PDZ domain alone. The structure of the PALS1-PSG–Crb-CT complex provides an atomic picture explaining the exquisitely specific PALS1–Crb interaction afforded by the PSG supramodule. Tempering the PSG supramodule conformation impairs PALS1-mediated cell-polarity establishment. We further show that formation of the PSG supramodule may be a general mechanism for forming highly specific MAGUK–target complexes.

Results

PALS1-PSG but Not the Isolated PDZ Domain Binds to Crb-CT with High Affinity. We first verified the PALS1–Crb-CT interaction using highly purified recombinant proteins. Analytical gel filtration chromatography and a quantitative binding assay showed that Crb-CT binds to PALS1-PDZ with a K_d of ∼6.0 μM (Fig. 1 *B* and *D*), an affinity unlikely to support the highly specific Crb–PALS1 complex formation. Interestingly, Crb-CT binds to PALS1-PSG with a K_d of ∼0.07 μM (Fig. 1 *C* and *E*), which is about 100-fold stronger than the isolated PALS1-PDZ. The binding affinity between PALS1-PSG and Crb-CT is also much stronger than the vast majority of reported interactions between PBMs and isolated PDZ domains (ref. 29 and references therein), thus pointing to a biochemical basis for the formation of the specific Crb–PALS1 complex required for cell polarity.

Overall Structure of the PALS1-PSG–Crb-CT Complex. To understand the molecular basis governing the specific PALS1–Crb interaction, we solved the structure of PALS1-PSG in complex with Crb-CT by X-ray crystallography. The PALS1-PSG used for the crystallization contains a deletion of a 50-residue HOOK region (residues 411–460) connecting the SH3 and GK domains (Fig. S1) to obtain complex crystals with high diffraction qualities, and the deletion has a minimal impact on Crb-CT binding (K_d of ∼0.12 μM). The crystal structure of the PALS1-PSG–Crb-CT complex was solved by single-wavelength anomalous dispersion using Se-Met derivatives and subsequently refined against a 2.95-Å native dataset (Table 1). Each asymmetric unit of the crystal contains two PALS1-PSG–Crb-CT complexes with essentially identical conformations (rmsd of 0.9 Å). The two PALS1-PSG–Crb-CT heterodimers interact with each other and are related by twofold symmetry. The last 17 residues of Crb-CT are clearly defined (Fig. S2). In each heterodimer, two distinct segments of the 17-residue Crb-CT bind to two separate sites of PALS1-PSG (Fig. 2*A*). The PBM binds to a channel formed by the extensively interacting PDZ and SH3 domains (Fig. 2*B*). Unexpectedly, an 8-residue fragment located between −9 and −16 of Crb-CT binds to the GK domain of PSG. To accommodate the short spacing between the two binding segments of Crb-CT, PALS1-PSG forms a U-shaped architecture with the tightly coupled PDZ and SH3 domains forming one arm and the GK domain forming the other, with minimal direct interaction between the two arms (i.e., little direct interaction between GK and PDZ/SH3). As observed in the SH3–GK tandem of DLGs (32), the flanking sequences of the GK domain form a pair of β-strands (pale green in Fig. 2 *A* and *D*), complementing and extending the SH3 domain. However, instead of bridging the SH3 and GK domains of DLGs intramolecularly, the pair of β-strands connects the SH3 core (green) and GK domain (light orange) from the two neighboring PSG molecules (Fig. 2 *C* and *D*). We note that the PALS1-PSG is a monomer in solution, indicating that the PALS1-PSG homodimer formed in the crystal may be induced by the binding of Crb-CT. A similar intermolecular interaction between SH3 and GK in MAGUKs has also been observed in DLG family MAGUKs (32, 33). The interdomain flexibility between the SH3 and GK domains has also been implicated by orientation differences between the two domains observed in the structures of different MAGUK SH3–GK tandems (32–35). Given the very few conformational restraints between the two conformers, PALS1-PSG (and possibly other MAGUK PSG tandems) may assume either the U shape or the shape of elongated conformers depending on its ligand-binding status.

The Binding of Crb-PBM to PALS1-PSG Involves Both the PDZ and SH3 Domains. Our complex structure reveals that the four strictly conserved Crb-PBM residues ("ERLI") form a short β-strand that fits snuggly into a semiclosed channel formed by PDZ and SH3 of PSG (Figs. 2*B* and 3*B*). Every residue of Crb-PBM is intimately involved in binding to PDZ and/or SH3 of PALS1-PSG (Fig. 3*A*). As in the canonical PDZ–PBM interactions, the very last residue of Crb, I(0), deeply inserts its side chain into the hydrophobic pocket of PALS1-PDZ, with its carboxyl group forming hydrogen bonds with the backbone of the GLGF loop. Importantly, the SH3 domain is also extensively involved in binding to the residues in

Table 1. Statistics of data collection and model refinement

Data collection		
Dataset	Native	Se-Met derivative
Space group	$P4_12_12$	$P4_12_12$
Unit cell parameters, Å	a = b = 111.9, c = 223.1	a = b = 112.5, c = 223.3
Resolution range, Å	50–2.95 (3.0–2.95)	50–3.4 (3.46–3.4)
No. of unique reflections	30,528 (1,488)	19,987 (982)
Redundancy	11.8 (12.7)	9.6 (9.8)
I/σ	33.9 (4.1)	38.2 (6.1)
Completeness, %	99.6 (100)	98.6 (97.3)
R_{merge}, %*	8.3 (76.1)	9.5 (60.0)
Structure refinement		
Resolution, Å	50–2.95 (3.05–2.95)	
R_{cryst}/R_{free}, %†	20.7 (27.7)/23.5 (30.4)	
Rmsd bonds, Å/angles, °	0.003/0.7	
Average B factor	90.7	
No. of protein atoms	6,022	
No. of water molecules	20	
No. of reflections		
Working set	28,898	
Test set	1,521	
Ramachandran plot, %		
Favored regions	96.3	
Allowed regions	3.7	
Outliers	0.0	

Numbers in parentheses represent the value for the highest resolution shell.

*$R_{merge} = \sum|I_i - I_m|/\sum I_i$, where I_i is the intensity of the measured reflection and I_m is the mean intensity of all symmetry-related reflections.

†$R_{cryst} = \Sigma||F_{obs}| - |F_{calc}||/\Sigma|F_{obs}|$, where F_{obs} and F_{calc} are observed and calculated structure factors. $R_{free} = \Sigma_T||F_{obs}| - |F_{calc}||/\Sigma_T|F_{obs}|$, where T is a test dataset of about 5% of the total reflections randomly chosen and set aside before refinement.

the −1 to −3 positions of Crb-PBM. L369^{SH3} and L403^{SH3}, together with P266, T270, and V284 from the PDZ domain, form an additional hydrophobic pocket for L(−1). E368^{SH3} forms a hydrogen bond with the backbone of the PBM and also interacts with the side chain of R(−2), which is in turn sandwiched by F318 and N315 in αA of the PDZ domain. E(−3) of Crb-PBM forms a pair of buried salt bridges with R282^{PDZ} and a buried hydrogen bond with T270^{PDZ}. The Crb-PBM–PALS1-PSG interaction is further strengthened by hydrogen bonds formed between atoms from the backbone of Crb-PBM and from backbones of PDZ βB and the βA′/B′ loop of SH3 (Fig. 3*A*). Thus, through the extensive interaction with both the PDZ and SH3 domains by using each of the four residues, Crb-PBM shows a very strong and specific interaction with PALS1-PSG, largely explaining why the PDZ domain alone is not sufficient to achieve high-affinity binding. The side chains of F318^{PDZ} and E368^{SH3} embrace and thus partially bury Crb-PBM (Fig. 2 *B* and *C*). Consistently, substitution of F318^{PDZ} with Ala weakens the binding by ∼20-fold (Fig. 3*C*). The above structural analysis provides a clear mechanistic explanation for the indispensable roles of both the SH3 and PDZ domains of PALS1 in binding to Crb.

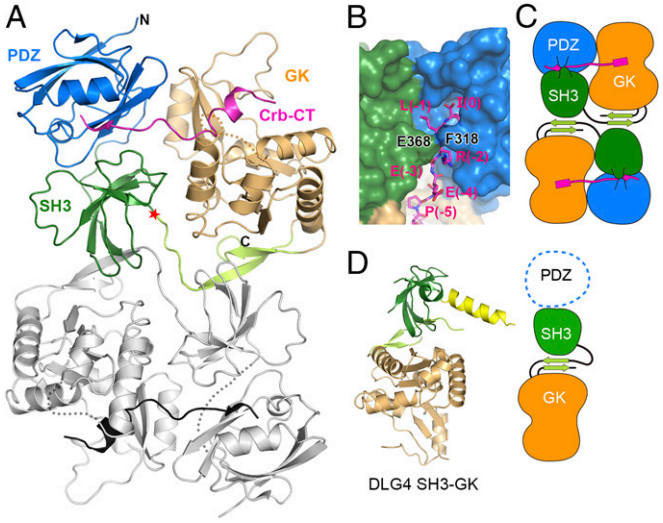

Fig. 2. Overall structure of the PALS1-PSG–Crb-CT complex. (*A*) Two PALS1-PSG–Crb-CT heterodimers form a dimer related by a twofold axis. The disordered loops are indicated by dotted lines. The deletion site in PALS1-PSG_ΔHOOK is denoted by a red star. (*B*) Surface representation of the Crb-PBM binding site in the PDZ–SH3 tandem. The surfaces are semitransparent to show that Crb-PBM is partially buried by two residues, F318 and E368, from the PDZ and SH3 domains, respectively. (*C*) Schematic cartoon showing the PALS1-PSG–Crb-CT interaction as well as the PSG interdomain interactions for the dimer of dimers in the crystal. (*D*) The SH3–GK tandem of DLG4 is shown with the SH3 aligned in the same view as that of PALS1. The cartoon shows the corresponding assembly mode for the SH3–GK tandem in DLG4.

Based on the above analysis, we hypothesized that tempering of the coupling between the SH3 and PDZ domains would impair the PALS1-PSG–Crb-CT interaction. To test this hypothesis, we substituted Asp386 with Lys and tested the mutant PALS1-PSG in binding to Crb-CT. Because Asp386^{SH3} and Arg282^{PDZ} form a pair of salt bridges that are away from the Crb-PBM–binding channel (Fig. 3*D*), the dramatically decreased binding of Crb-CT to D386K–PASL1-PSG likely results from the mutation-induced impairment of the SH3–PDZ coupling (Fig. 3*C*).

The GK Domain Enhances the Binding of PALS1 to Crb-CT. An unexpected finding in the structure of the PALS1-PSG–Crb-CT complex is that an 8-residue fragment upstream of the PBM [residues L(−9) to R(−16), termed the GBM] in Crb-CT directly binds to PALS1-GK (Fig. 4*A*). Interestingly, the GK–GBM interaction mimics the phosphorylation-dependent target binding

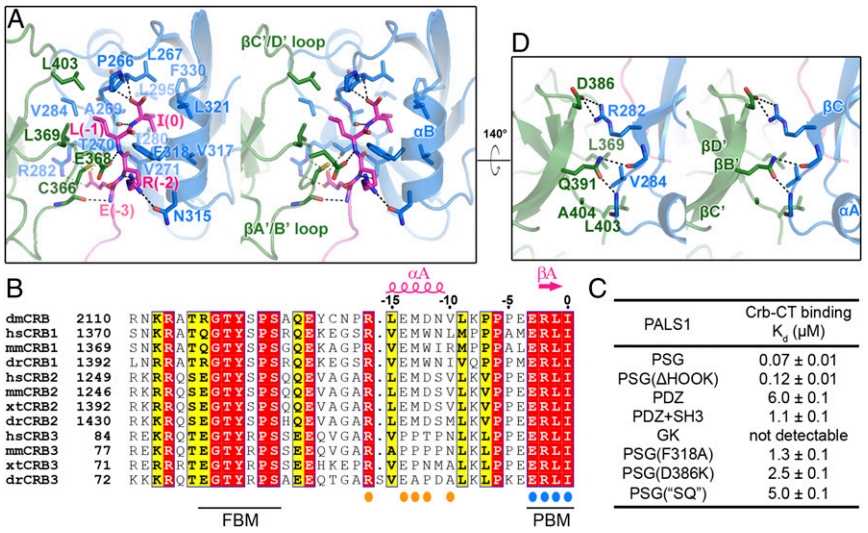

Fig. 3. Molecular details of PDZ–SH3 coupling. (*A*) Stereoview of the binding of Crb-PBM to PALS1 PDZ–SH3. Salt bridges and hydrogen bonds are indicated by dashed lines. (*B*) Sequence alignment of the cytoplasmic regions of different Crb proteins (dm, *Drosophila melanogaster*; dr, *Danio rerio*; hs, *Homo sapiens*; mm, *Mus musculus*; xt, *Xenopus tropicalis*). In this alignment, residues that are absolutely conserved and highly conserved are highlighted in red and yellow, respectively. The residues involved in the PDZ–PBM and GK–GBM interactions are indicated by blue and orange circles, respectively. (*C*) ITC-based measurements summarizing the binding affinities of Crb-CT to PALS1-PSG and several of its mutants characterized in the study. (*D*) Molecular details of the PDZ–SH3 interdomain interaction.

of DLG GK domains, such as the interaction between DLG1-GK and phosphor-LGN shown in Fig. 4*B* (36). Similar to p-LGN, the PALS1-GK–bound GBM adopts a short helical conformation and employs E(−14) to mimic the p-Ser in LGN to interact with two highly conserved Arg residues (R516 and R519) in the GK domain. Additionally, D(−12) in the GBM forms a salt bridge with $R496^{GK}$. Deletion of the GK domain from PALS1-PSG decreased the binding of Crb-CT to PALS1 by ∼15-fold (Fig. 3*C*). Nonetheless, the GK domain alone shows no detectable binding to Crb-CT (Fig. 3*C*), indicating that the GK domain plays a supporting role in aiding the PDZ/SH3 domain-mediated Crb-CT binding of PALS1-PSG. Supporting the above structural analysis, the binding between mammalian Crb3-CT and PALS1-PSG is a few-fold weaker than Crb1-CT or *Drosophila* Crb-CT (Fig. S3), as the −14 residue in mammalian Crb3-CT is a Pro instead of a Glu (Fig. 3*B*).

The PSG Tandem of PALS1 Is Essential for Proper Cystogenesis of Madin–Darby Canine Kidney Cells. We next used Madin–Darby canine kidney (MDCK) cystogenesis as a model to test the role of the high-affinity interaction between PALS1 and Crb afforded by the PALS1-PSG supramodule. We generated stable cell lines each expressing siRNA-resistant wild-type PALS1 (WT-PALS1) and two of its mutants, PALS1-PDZ (PALS1 with the SH3–GK tandem deleted) and PALS1-D386K (full-length PALS1 with the PDZ–SH3 coupling impaired). Consistent with an earlier report (31), lentivirus-mediated knockdown of endogenous PALS1 is efficient (Fig. S4*A*). Exogenously expressed WT-PALS1 and PALS1-D386K mutant were at a comparable level, and PALS1-PDZ was at a higher level than WT-PALS1 (Fig. S4*B*). Fitting with our structural analysis,

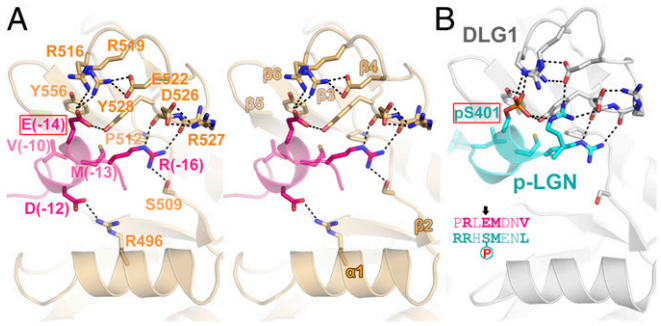

Fig. 4. Crb-CT–PALS1-GK interaction. (*A*) Molecular details showing how Crb-GBM interacts with PALS1-GK. (*B*) The phosphorylation-dependent interaction between the phosphor-LGN peptide and the DLG1 GK domain (36). (*Inset*) Sequence alignment of the GK-binding peptides from Crb-CT and LGN. The arrow points to the phospho-Ser–mimicking residue Glu.

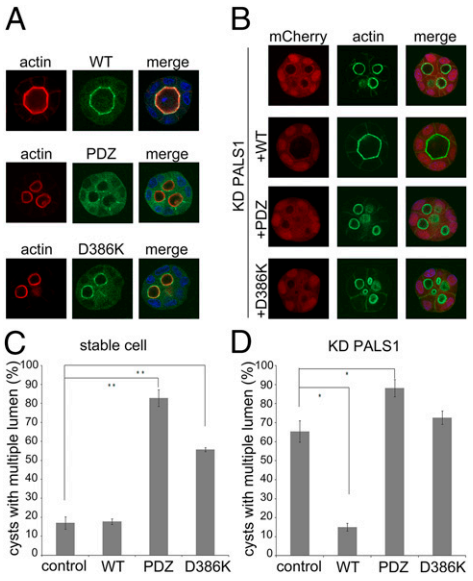

Fig. 5. PSG tandem of PALS1 is essential for its role in apical–basal cell polarity in MDCK cysts. (*A*) MDCK cells stably expressing the Venus-tagged wild-type PALS1 (WT), PALS1 mutant with the SH3–GK tandem deleted (PDZ), and PALS1 PDZ–SH3 uncoupling mutant (D386K) were cultured in Matrigel. Cysts were fixed and stained with rhodamine-conjugated phalloidin (red), anti-GFP antibody (green) against Venus, and DNA dye (blue), respectively. (*B*) Lentivirus-mediated knockdown of endogenous PALS1 (KD-PALS1) leads to defective cystogenesis, as indicated by the abnormal multilumen formation, and such defects can be rescued by expressing shRNA-resistant WT-PALS1 (top two panels). Knockdown of endogenous PALS1 led to more severe cystogenesis defects in cells stably expressing shRNA-resistant PALS1-PDZ or PALS1-D386K (bottom two panels). Control MDCK cells (*Top*) and MDCK cells stably expressing WT-PALS1, PALS1-PDZ, or PALS1-D386K were transduced by lentiviruses expressing mCherry (red) and shRNA against canine PALS1. mCherry-expressing cells are considered virus-transduced, PALS1 knockdown cells. Virus-transduced cells were cultured in Matrigel for cystogenesis. Cysts were fixed and stained with Alexa 488-conjugated phalloidin (green) and DNA dye (blue). (*C* and *D*) Quantification of the cysts with abnormal lumen formation in *A* and *B*, respectively. Values are mean ± SD from three independent experiments ($n > 100$ for each group). $^{*}P < 0.01$, $^{**}P < 0.001$.

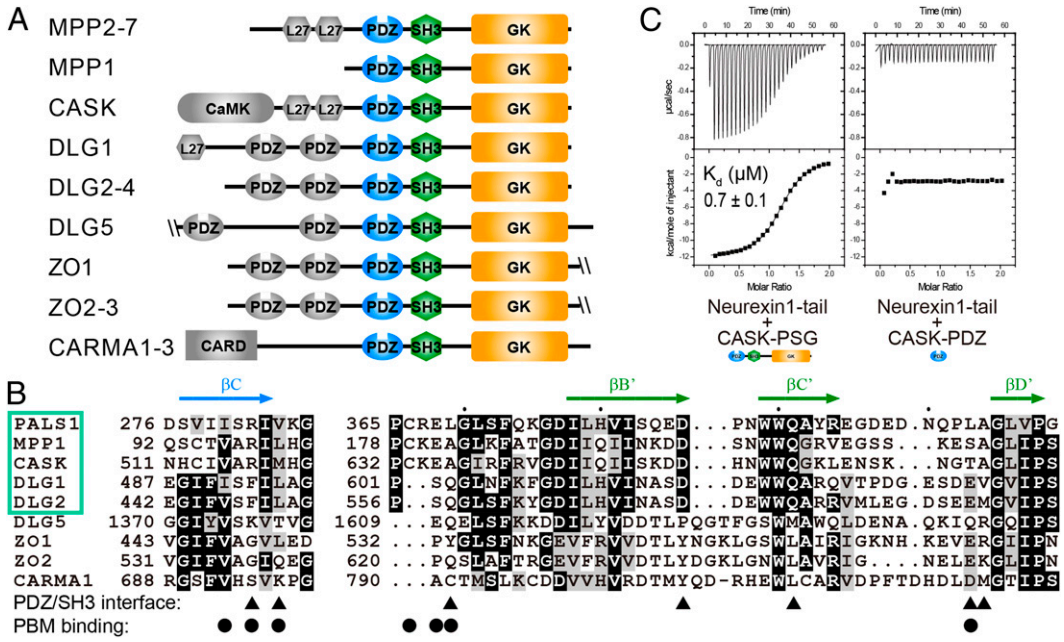

Fig. 6. Other MAGUKs may also form PSG supramodules. (*A*) Schematic diagrams showing the domain organization of MAGUKs. (*B*) Sequence alignment showing the residues in the PDZ–SH3 interface among PALS1 and other MAGUKs. Residues involved in the PDZ–SH3 coupling and Crb-PBM binding are highlighted with triangles and circles, respectively. (*C*) ITC-based measurements comparing the binding of the neurexin tail to CASK-PSG and CASK-PDZ.

neither of the PALS1 mutants localized properly, and both caused defective cystogenesis when expressed in MDCK cells. In contrast, expression of WT-PALS1 had little impact on proper cyst formation (Fig. 5 *A* and *C*). Additionally, lentivirus-mediated stable knockdown of endogenous PALS1 in MDCK cells led to cystogenesis defects, which could be fully rescued when shRNA-resistant WT-PALS1 was expressed (Fig. 5 *B* and *D*). In contrast, depletion of endogenous PALS1 in cells expressing either of the PALS1 mutants induced more severe defects in cystogenesis characterized by a significantly higher portion of cysts containing multiple lumens (Fig. 5 *B* and *D*). The above data confirm that the integral PSG structural supramodule of PALS1 is essential for its function in apical–basal cell polarity in the MDCK model.

Formation of the PDZ–SH3–GK Supramodule in Other MAGUKs. MAGUKs are a large family of scaffold proteins that play essential roles in cell–cell communications, cell-polarity maintenance, synaptic formation, and cellular signal transductions (36, 37). All MAGUKs, except for MAGI, contain a PDZ–SH3–GK core element (Fig. 6*A*), raising a possibility that the three domains in the tandem may function synergistically in binding to their respective targets (34, 38, 39). Earlier, the SH3 domain of ZO1-PSG had been shown to enhance the PDZ domain-mediated binding to connexin45 (34). However, the interaction between PDZ and SH3 in ZO1 is totally different from that in PALS1 (Fig. S5). As such, ZO1-SH3 has very limited contact with the connexin45 PBM using its βB′/C′ loop, instead of the intimate involvement of PALS1-SH3 in binding to Crb-PBM using its βA′/B′ loop (Fig. S5 *C* and *D*). Accordingly, the interaction between ZO1-PSG and the connexin45 tail is very modest [K_d of ∼8 μM (34)]. By aligning the PSG-containing MAGUK proteins, we found that the residues forming the PDZ–SH3 interface in PALS1 are conserved in MPPs, CASK, and DLG1–4 (Fig. 6*B* and Fig. S6), raising a possibility that these MAGUKs may also use their respective PSG tandem to interact with targets. To test this possibility, we compared the binding of the isolated PDZ and the PSG tandem of CASK in binding to the C-terminal tail of neurexin, a reported presynaptic target of CASK (40). Interestingly, the isolated CASK-PDZ has no detectable binding to the neurexin tail. In contrast, the CASK-PSG binds to the neurexin tail with a K_d of ∼0.7 μM (Fig. 6*C*). The above data provide another example showing the critical role of the PSG tandem of a MAGUK in specifically binding to its target, although the mechanistic details of the interaction remain to be elucidated.

Although several MAGUKs such as MPPs, CASK, and DLGs may share similar structural mechanisms in their PDZ–SH3 couplings, the amino acid residues involved in target binding (e.g., the residues in their βA′/B′ loops) do not completely overlap (Fig. 6*B*). Thus, the PDZ–SH3 duals of these MAGUKs are likely to have target-binding specificities. Indeed, replacing a 4-residue fragment ("CREL") in the βA′/B′ loop of PALS1 SH3 with the corresponding sequence ("SQ") from DLG-SH3 (Fig. 6*B*) caused an ∼100-fold affinity decrease of PALS1-PSG's binding to Crb-CT [denoted PSG("SQ") in Fig. 3*C*]. Thus, formation of the PSG supramodule not only enhances affinities but can also increase specificities for MAGUKs in recognizing their respective targets.

Discussion

PDZ domain proteins as well as their targets are highly abundant both in their numbers and quantities in metazoans. Frequent enrichment of PDZ proteins and their targets in constricted regions of cellular processes such as polarized membrane domains and cell–cell junctions often results in their coexistence in a confined space with high concentrations. Most of the reported PDZ domain and target interactions in vitro are of modest affinity and specificity (ref. 29 and references therein). If such promiscuous PDZ–target interactions were also to occur in vivo and also considering that many PDZ proteins contain multiple PDZ domains, one would expect that the PDZ protein-mediated complex assemblies/networks would be highly interconnected and messy. Obviously, such "glue"-style PDZ–target interactions should not be the real picture in living cells. Consistently, numerous in vivo studies have revealed that PDZ domain proteins often form very specific functional complexes. The best examples are perhaps the three master cell-polarity regulatory complexes: Crb–PALS1–PATJ, PAR3–PAR6–aPKC, and DLG–Lgl–Scribble. Each of the three complexes contains multiple PDZ domains, and yet the PDZ domains of these

complexes have to bind to distinct targets to fulfill their distinct roles in cell polarity. We demonstrate here that the PDZ domain of PALS1 physically interacts with its connected SH3/GK domains to form a structural supramodule, providing a platform for PALS1's functional partner Crb to bind with high specificity and affinity (K_d of ~70 nM) over other reported binders such as the PAR6 C-terminal tail (K_d of a few micromolar) (41, 42). We further demonstrate that another MAGUK, CASK, also requires its PSG tandem to bind to its partner neurexin. In general, it is perhaps the norm rather than the exception that a PDZ domain often functions together with its extension sequences or neighboring domain(s) to engage its specific target(s) in living cells (29).

In addition to its determinant role in apical–basal cell polarity, the Crb complex has also been shown to interact with the Hippo pathway to regulate cell growth (16–18). It is interesting to note that the FBM of Crb-CT is completely spared from the Crb–PALS1 complex (Fig. 3). Thus, in theory, the Crb complex can directly engage the Hippo signaling pathway via Crb-CT. It has been reported that the FERM domain-containing protein Expanded functions as a mediator between Crb and the Hippo pathway in *Drosophila* (17). However, mammals do not contain the Expanded counterpart (43). Identification of the partner of Crb-FBM in mammals will be important to connect the two pathways regulating cell growth and cell polarity. Crb-CT may function as a switch for these two distinct but closely related cellular processes.

Materials and Methods

All proteins used in this study were expressed in *Escherichia coli* BL21(DE3) and purified by affinity chromatography followed by size-exclusion chromatography. Crystals were obtained by the hanging drop vapor diffusion method at 16 °C. An extended methods section describing protein preparation, crystallization, structure determination, and cell biology and biochemical assays can be found in *SI Materials and Methods*.

ACKNOWLEDGMENTS. We thank Shanghai Synchrotron Radiation Facility BL17U for X-ray beam time. We are grateful to Dr. Ian Macara (Vanderbilt University) for providing the anti-Pals1 antibody. This work was supported by grants from The Research Grants Council (RGC) of Hong Kong (663811, 663812, 664113, AoE/M09/12, and T13-607/12R to M.Z.), Asian Fund for Cancer Research, and the National Institutes of Health (GM079506 to Q.D.). M.Z. is a Kerry Holdings Professor in Science and a Senior Fellow of the Institute for Advanced Study at Hong Kong University of Science and Technology.

1. Tepass U (2012) The apical polarity protein network in *Drosophila* epithelial cells: Regulation of polarity, junctions, morphogenesis, cell growth, and survival. *Annu Rev Cell Dev Biol* 28:655–685.
2. Rodriguez-Boulan E, Macara IG (2014) Organization and execution of the epithelial polarity programme. *Nat Rev Mol Cell Biol* 15(4):225–242.
3. Martin-Belmonte F, Perez-Moreno M (2012) Epithelial cell polarity, stem cells and cancer. *Nat Rev Cancer* 12(1):23–38.
4. Margolis B, Borg JP (2005) Apicobasal polarity complexes. *J Cell Sci* 118(Pt 22): 5157–5159.
5. Knust E, Bossinger O (2002) Composition and formation of intercellular junctions in epithelial cells. *Science* 298(5600):1955–1959.
6. Tepass U, Tanentzapf G, Ward R, Fehon R (2001) Epithelial cell polarity and cell junctions in *Drosophila*. *Annu Rev Genet* 35:747–784.
7. Bulgakova NA, Knust E (2009) The Crumbs complex: From epithelial-cell polarity to retinal degeneration. *J Cell Sci* 122(Pt 15):2587–2596.
8. Nance J, Zallen JA (2011) Elaborating polarity: PAR proteins and the cytoskeleton. *Development* 138(5):799–809.
9. Suzuki A, Ohno S (2006) The PAR-aPKC system: Lessons in polarity. *J Cell Sci* 119(Pt 6): 979–987.
10. Bilder D (2004) Epithelial polarity and proliferation control: Links from the *Drosophila* neoplastic tumor suppressors. *Genes Dev* 18(16):1909–1925.
11. Tepass U, Theres C, Knust E (1990) crumbs encodes an EGF-like protein expressed on apical membranes of *Drosophila* epithelial cells and required for organization of epithelia. *Cell* 61(5):787–799.
12. Tepass U (1996) Crumbs, a component of the apical membrane, is required for zonula adherens formation in primary epithelia of *Drosophila*. *Dev Biol* 177(1):217–225.
13. Pocha SM, Knust E (2013) Complexities of Crumbs function and regulation in tissue morphogenesis. *Curr Biol* 23(7):R289–R293.
14. Wodarz A, Grawe F, Knust E (1993) CRUMBS is involved in the control of apical protein targeting during *Drosophila* epithelial development. *Mech Dev* 44(2-3):175–187.
15. Wodarz A, Hinz U, Engelbert M, Knust E (1995) Expression of crumbs confers apical character on plasma membrane domains of ectodermal epithelia of *Drosophila*. *Cell* 82(1):67–76.
16. Chen CL, et al. (2010) The apical-basal cell polarity determinant Crumbs regulates Hippo signaling in *Drosophila*. *Proc Natl Acad Sci USA* 107(36):15810–15815.
17. Ling C, et al. (2010) The apical transmembrane protein Crumbs functions as a tumor suppressor that regulates Hippo signaling by binding to Expanded. *Proc Natl Acad Sci USA* 107(23):10532–10537.
18. Varelas X, et al. (2010) The Crumbs complex couples cell density sensing to Hippo-dependent control of the TGF-β-SMAD pathway. *Dev Cell* 19(6):831–844.
19. Klebes A, Knust E (2000) A conserved motif in Crumbs is required for E-cadherin localisation and zonula adherens formation in *Drosophila*. *Curr Biol* 10(2):76–85.
20. Klose S, Flores-Benitez D, Riedel F, Knust E (2013) Fosmid-based structure-function analysis reveals functionally distinct domains in the cytoplasmic domain of *Drosophila* Crumbs. *G3 (Bethesda)* 3(2):153–165.
21. Sotillos S, Díaz-Meco MT, Caminero E, Moscat J, Campuzano S (2004) DaPKC-dependent phosphorylation of Crumbs is required for epithelial cell polarity in *Drosophila*. *J Cell Biol* 166(4):549–557.
22. Laprise P, et al. (2006) The FERM protein Yurt is a negative regulatory component of the Crumbs complex that controls epithelial polarity and apical membrane size. *Dev Cell* 11(3):363–374.
23. Roh MH, et al. (2002) The Maguk protein, Pals1, functions as an adapter, linking mammalian homologues of Crumbs and Discs Lost. *J Cell Biol* 157(1):161–172.
24. Bulgakova NA, Kempkens O, Knust E (2008) Multiple domains of Stardust differentially mediate localisation of the Crumbs-Stardust complex during photoreceptor development in *Drosophila*. *J Cell Sci* 121(Pt 12):2018–2026.
25. Bachmann A, Schneider M, Theilenberg E, Grawe F, Knust E (2001) *Drosophila* Stardust is a partner of Crumbs in the control of epithelial cell polarity. *Nature* 414(6864): 638–643.
26. Hong Y, Stronach B, Perrimon N, Jan LY, Jan YN (2001) *Drosophila* Stardust interacts with Crumbs to control polarity of epithelia but not neuroblasts. *Nature* 414(6864): 634–638.
27. Stiffler MA, et al. (2007) PDZ domain binding selectivity is optimized across the mouse proteome. *Science* 317(5836):364–369.
28. Tonikian R, et al. (2008) A specificity map for the PDZ domain family. *PLoS Biol* 6(9): e239.
29. Ye F, Zhang M (2013) Structures and target recognition modes of PDZ domains: Recurring themes and emerging pictures. *Biochem J* 455(1):1–14.
30. Tepass U, Knust E (1993) crumbs and stardust act in a genetic pathway that controls the organization of epithelia in *Drosophila melanogaster*. *Dev Biol* 159(1):311–326.
31. Wang Q, Chen XW, Margolis B (2007) PALS1 regulates E-cadherin trafficking in mammalian epithelial cells. *Mol Biol Cell* 18(3):874–885.
32. McGee AW, et al. (2001) Structure of the SH3-guanylate kinase module from PSD-95 suggests a mechanism for regulated assembly of MAGUK scaffolding proteins. *Mol Cell* 8(6):1291–1301.
33. Shin H, Hsueh YP, Yang FC, Kim E, Sheng M (2000) An intramolecular interaction between Src homology 3 domain and guanylate kinase-like domain required for channel clustering by postsynaptic density-95/SAP90. *J Neurosci* 20(10):3580–3587.
34. Pan L, Chen J, Yu J, Yu H, Zhang M (2011) The structure of the PDZ3-SH3-GuK tandem of ZO-1 protein suggests a supramodular organization of the membrane-associated guanylate kinase (MAGUK) family scaffold protein core. *J Biol Chem* 286(46):40069–40074.
35. McGee AW, et al. (2004) Calcium channel function regulated by the SH3-GK module in beta subunits. *Neuron* 42(1):89–99.
36. Zhu J, et al. (2011) Guanylate kinase domains of the MAGUK family scaffold proteins as specific phospho-protein-binding modules. *EMBO J* 30(24):4986–4997.
37. Funke L, Dakoji S, Bredt DS (2005) Membrane-associated guanylate kinases regulate adhesion and plasticity at cell junctions. *Annu Rev Biochem* 74:219–245.
38. Zhang J, Lewis SM, Kuhlman B, Lee AL (2013) Supertertiary structure of the MAGUK core from PSD-95. *Structure* 21(3):402–413.
39. McCann JJ, et al. (2012) Supertertiary structure of the synaptic MAGuK scaffold proteins is conserved. *Proc Natl Acad Sci USA* 109(39):15775–15780.
40. Hata Y, Butz S, Südhof TC (1996) CASK: A novel dlg/PSD95 homolog with an N-terminal calmodulin-dependent protein kinase domain identified by interaction with neurexins. *J Neurosci* 16(8):2488–2494.
41. Kempkens O, et al. (2006) Computer modelling in combination with in vitro studies reveals similar binding affinities of *Drosophila* Crumbs for the PDZ domains of Stardust and DmPar-6. *Eur J Cell Biol* 85(8):753–767.
42. Lemmers C, et al. (2004) CRB3 binds directly to Par6 and regulates the morphogenesis of the tight junctions in mammalian epithelial cells. *Mol Biol Cell* 15(3):1324–1333.
43. Bossuyt W, et al. (2014) An evolutionary shift in the regulation of the Hippo pathway between mice and flies. *Oncogene* 33(10):1218–1228.